

# A Computational Theory of Spike-Timing Dependent Plasticity: Achieving Robust Neural Responses via Conditional Entropy Minimization\*

Sander Bohte<sup>1</sup>   Michael C. Mozer<sup>2</sup>  
S.M.Bohte@cwi.nl   mozer@cs.colorado.edu

<sup>1</sup> *CWI, The Netherlands Centre for Mathematics and Computer Science  
P.O. Box 94079, 1090 GB Amsterdam, The Netherlands*

<sup>2</sup> *Department of Computer Science, University of Colorado  
Boulder, CO 80309-0430, United States*

## ABSTRACT

Experimental studies have observed synaptic potentiation when a presynaptic neuron fires shortly before a postsynaptic neuron, and synaptic depression when the presynaptic neuron fires shortly after. The dependence of synaptic modulation on the precise timing of the two action potentials is known as *spike-timing dependent plasticity* or *STDP*. We derive STDP from a simple computational principle: synapses adapt so as to minimize the postsynaptic neuron's variability to a given presynaptic input, causing the neuron's output to become more reliable in the face of noise. Using an entropy-minimization objective function and the biophysically realistic spike-response model of Gerstner (2001), we simulate neurophysiological experiments and obtain the characteristic STDP curve along with other phenomena including the reduction in synaptic plasticity as synaptic efficacy increases. We compare our account to other efforts to derive STDP from computational principles, and argue that our account provides the most comprehensive coverage of the phenomena. Thus, reliability of neural response in the face of noise may be a key goal of unsupervised cortical adaptation.

*2000 Mathematics Subject Classification:* 82C32, 68T05, 68T10, 68T30, 92B20.

*2000 ACM Computing Classification System:* C.1.3, F.1.1, I.2.6, I.5.1.

*Keywords and Phrases:* spike timing dependent plasticity (STDP), spike response model, stochastic thresholds, spiking neurons, minimal entropy.

*Note:* A short version of this paper has been presented at the Seventeenth Conference on Advances in Neural Information Processing (NIPS), 2004, Vancouver, Canada.

## 1. INTRODUCTION

Experimental studies have observed synaptic potentiation when a presynaptic neuron fires shortly before a postsynaptic neuron, and synaptic depression when the presynaptic neuron fires shortly after (Markram, Lübke, Frotscher, & Sakmann, 1997; Bell, Han, Sugawara, & Grant, 1997; Zhang, Tao, Holt, Harris, & Poo, 1998; G.-q. Bi & Poo, 1998; Debanne, Gähwiler, & Thompson, 1998; Feldman, 2000; Sjöström, Turrigiano, & Nelson, 2001; Nishiyama, Hong, Mikoshiba, Poo, & Kato, 2000). The dependence of synaptic modulation on the precise timing of the two action potentials, known as *spike-timing dependent plasticity* or *STDP*, is depicted in Figure 1. Typically, plasticity is observed only when the presynaptic and postsynaptic spikes occur within a 20–30 ms time window, and the transition from potentiation to depression is very rapid. The effects are long lasting, and are therefore referred to as long-term potentiation (LTP) and depression (LTD). An important observation is that the relative magnitude of the LTP component of STDP decreases with increased synaptic efficacy between presynaptic and postsynaptic neuron, whereas the magnitude of LTD remains roughly constant (G.-q. Bi & Poo, 1998). This finding has led to the suggestion that the LTP component of STDP might best be modeled as additive, whereas the LTD component is better modeled as being multiplicative

---

\*This paper has been submitted for publication. This is a preprint, CWI Technical Report Number SEN E0505.

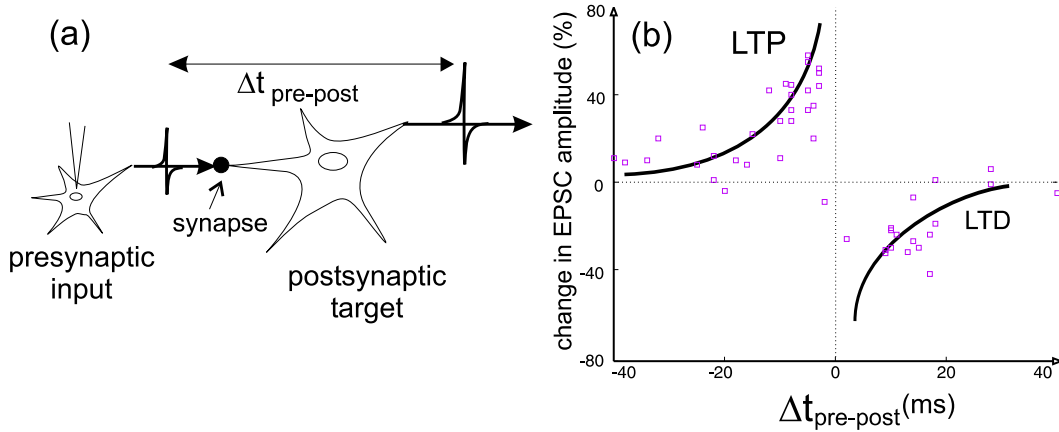


Figure 1: (a) Measuring STDP experimentally: presynaptic and postsynaptic spike pairs are repeatedly induced at a fixed interval  $\Delta t_{\text{pre-post}}$ , and the resulting change to the strength of the synapse is assessed; (b) change in synaptic strength after repeated spike pairing as a function of the difference in time between the presynaptic and postsynaptic spikes: a presynaptic before postsynaptic spike induces LTP, postsynaptic before presynaptic LTD (data redrawn from Zhang *et al.*, 1998). We have superimposed an exponential fit of LTP and LTD.

(Kepecs, van Rossum, Song, & Tegner, 2002). For detailed reviews of STDP, see (G.-q. Bi & Poo, 2001; Roberts & Bell, 2002; Dan & Poo, 2004).

Because these intriguing findings appear to describe a fundamental learning mechanism in the brain, a flurry of models have been developed that focus on different aspects of STDP. A number of studies focus on biochemical models that explain the underlying mechanisms giving rise to STDP: (Senn, Markram, & Tsodyks, 2000; G.-Q. Bi, 2002; Karmarkar, Najarian, & Buonomano, 2002; Saudargiene, Porr, & Wörgötter, 2004; Porr & Wörgötter, 2003). Many researchers have also focused on models that explore the consequences of a STDP-like learning rules in an ensemble of spiking neurons, i.e. (Gerstner, Kempter, van Hemmen, & Wagner, 1996; Kempter, Gerstner, & van Hemmen, 1999; Song, Miller, & Abbott, 2000; van Rossum, Bi, & Turrigiano, 2000; Kempter, Gerstner, & van Hemmen, 2001; Izhikevich & Desai, 2003; Abbott & Gerstner, 2004; Burkitt, Meffin, & Grayden, 2004; Shon, Rao, & Sejnowski, 2004; Legenstein, Naeger, & Maass, n.d.), a comprehensive review of the different types and conclusions can be found in Porr and Wörgötter (2003). Finally, a recent trend is to propose models that provide fundamental computational justifications for STDP. This article proposes a novel justification and we explore the consequences of this justification in detail.

Most commonly, STDP is viewed as a type of asymmetric Hebbian learning with a temporal dimension. However, this perspective is hardly a fundamental computational rationale, and one would hope that such an intuitively sensible learning rule would emerge from a first-principle computational justification.

Several researchers have tried to derive a learning rule yielding STDP from first principles. Dayan and Häusser (2004) show that STDP can be viewed as an optimal noise-removal filter for certain noise distributions. However, even small variation from these noise distributions yield quite different learning rules, and the noise statistics of biological neurons are unknown. Similarly, Porr and Wörgötter (2003) propose an unsupervised learning rule based on the correlation of bandpass-filtered inputs with the derivative of the output, and show that the weight change rule is qualitatively similar to STDP.

Hopfield and Brody (2004) derive learning rules that implement ongoing network self-repair. In some circumstances, a qualitative similarity to STDP is found, but the shape of the learning rule depends on both network architecture and task. Eisele (private communication) has shown that an

STDP-like learning rule can be derived from the goal of maintaining the relevant connections in a network.

Rao and Sejnowski (1999, 2001) suggest that STDP may be related to prediction, in particular to **temporal difference (TD) learning**. They argue that STDP emerges when a neuron attempts to predict its membrane potential at some time  $t$  from the potential at time  $t - \Delta t$ . As Dayan (2002) points out however, temporal difference learning depends on an estimate of the prediction error, which will be very hard to obtain. Rather, a quantity that might be called an “activity difference” can be computed, and the learning rule is then better characterized as a “correlational learning rule between the stimuli, and the *differences* in successive outputs” (Dayan, 2002) (see also Porr and Wörgötter (2003), Appendix B). Furthermore, Dayan argues that for true prediction, the model has to show that the learning rule works for biologically realistic timescales. The qualitative nature of the modeling makes it unclear whether a quantitative fit can be obtained. Lastly, the derived difference rule is inherently unstable, as it does not impose any bounds on synaptic efficacies; also, STDP emerges only for a narrow range of  $\Delta t$  values.

**Chechik (2003) relates STDP to information theory via maximization of mutual information between input and output spike trains.** This approach derives the LTP portion of STDP, but fails to yield the LTD portion. Nonetheless, an information-theoretic approach is quite elegant and has proven valuable in explaining other neural learning phenomena (e.g., Linsker, 1989).

The account we describe in this paper also exploits an information-theoretic approach. We are not the only ones to appreciate the elegance of information-theoretic accounts. In parallel with a preliminary presentation of our work at the NIPS 2004 conference, two quite similar information-theoretic accounts also appeared (Bell & Parra, 2005; Toyozumi, Pfister, Aihara, & Gerstner, 2005). It will be easiest to explain the relationship of these accounts to our own once we have presented ours.

The computational approaches of Chechik, Dayan & Häusser, and Porr & Wörgötter are all premised on a rate-based neuron model that disregards the relative timing of spikes. It seems quite odd to argue for STDP using neural firing *rate*: if spike timing is irrelevant to information transmission, then STDP is likely an artifact and is not central to understanding mechanisms of neural computation. Further, as in Dayan and Häusser (2004) note, because STDP is not quite additive in the case of multiple input or output spikes that are near in time (Froemke & Dan, 2002), one should consider interpretations that are based on individual spikes, not aggregates over spike trains.

**In this paper, we present an alternative theoretical motivation for STDP from a spike-based neuron model that takes the specific times of spikes into account.** We conjecture that a fundamental objective of cortical computation is to achieve *reliable* neural responses, that is, **neurons should produce the identical response—both in the number and timing of spikes—given a fixed input spike train.** Reliability is an issue if neurons are affected by noise influences, because noise leads to variability in a neuron’s dynamics and therefore in its response. Minimizing this variability will reduce the effect of noise and will therefore increase the informativeness of the neuron’s output signal. The source of the noise is not important; it could be intrinsic to a neuron (e.g., a time-varying threshold) or it could originate in unmodeled external sources that cause fluctuations in the membrane potential uncorrelated with a particular input.

**We are not suggesting that increasing neural reliability is the *only* objective of learning. If it were, a neuron would do well to shut off and give no response regardless of the input.** Rather, reliability is but one of many objectives that learning tries to achieve. This form of unsupervised learning must, of course, be complemented by supervised and reinforcement learning objectives that allow an organism to achieve its goals and satisfy drives.

We derive STDP from the following computational principle: **synapses adapt so as to minimize the entropy of the postsynaptic neuron’s output in response to a given presynaptic input.** In our simulations, we follow the methodology of neurophysiological experiments. This approach leads to a detailed fit to key experimental results. We model not only the shape (sign and time course) of the STDP curve, but also the fact that potentiation of a synapse depends on the efficacy of the synapse—it decreases with increased efficacy. In addition to fitting these key STDP phenomena, the model allows

us to make predictions regarding the relationship between properties of the neuron and the shape of the STDP curve. The detailed quantitative fit to data makes our work unique among first-principle computational accounts.

Before delving into the details of our approach, we attempt to give a basic intuition about the approach. Noise in spiking neuron dynamics leads to variability in the number and timing of spikes. Given a particular input, one spike train might be more likely than others, but the output is non-deterministic. By the entropy-minimization principle, adaptation should reduce the likelihood of these other possibilities. To be concrete, consider a particular experimental paradigm. In Zhang et al. (1998), a presynaptic neuron is identified with a weak synapse to a post neuron, such that this presynaptic input is unlikely to cause the postsynaptic neuron to fire. However, the postsynaptic neuron can be induced to fire via a second presynaptic connection. In a typical trial, the presynaptic neuron is induced to fire a single spike, and with a variable delay, the postsynaptic neuron is also induced to fire (typically) a single spike. To increase the likelihood of the observed postsynaptic response other response possibilities must be suppressed.

With presynaptic input preceding the postsynaptic spike, the most likely alternative response is no output spikes at all. Increasing the synaptic connection weight should then reduce the possibility of this alternative response. With presynaptic input following the postsynaptic spike, the most likely alternative response is a second output spike. Decreasing the synaptic connection weight should reduce the possibility of this alternative response. Because both of these alternatives become less likely as the lag between pre and post spikes is increased, one would expect that the magnitude of synaptic plasticity diminishes with the lag, as is observed in the STDP curve.

Our approach to reducing response variability given a particular input pattern involves computing the gradient of synaptic weights with respect to a differentiable model of spiking neuron behavior. We use the Spike Response Model (SRM) of Gerstner (2001) with a stochastic threshold, where the stochastic threshold models fluctuations of the membrane potential or the threshold outside of experimental control. For the stochastic SRM, the response probability is differentiable with respect to the synaptic weights, allowing us to calculate the entropy gradient with respect to the weights. Learning is presumed to take a gradient step to reduce the entropy. In modeling neurophysiological experiments, we demonstrate that this learning rule yields the typical STDP curve. We can predict the relationship between the exact shape of the STDP curve and physiologically measurable parameters, and we show that our results are robust to the choice of the few free parameters of the model.

In parallel with our work, two other groups of authors have proposed explanations of STDP in terms of neurons maximizing an information-theoretic measure—in their case, the mutual information between input and output spike trains—for the Spike-Response Model (Bell & Parra, 2005; Toyozumi et al., 2005). Toyozumi et al. (2005) maximize mutual information the input and output between a pool of presynaptic neurons and a single postsynaptic output neuron whereas Bell and Parra (2005) maximize information between a pool of (possibly correlated) presynaptic neurons and a pool of postsynaptic neurons. Bell and Parra (2005) use a deterministic SRM model and do not obtain the LTD component of STDP. As we will show, obtaining LTD critically depends on a stochastic neural response. In the derivation of Toyozumi et al. (2005), LTD is attributed to the refractoriness of the spiking neuron, where they use questionably strong and enduring refractoriness. In our framework, refractoriness suppresses noise in the neuron after spiking, and we show that in our simulations strong refraction in fact diminishes the LTD component of STDP.

Furthermore, the mathematical derivation of Toyozumi et al. (2005) is valid only for an essentially constant membrane potential with small fluctuations, a condition which is clearly violated in experimental conditions studied by neurophysiologists. It is unclear whether the derivation would hold under more realistic conditions.

Neither of these approaches thus far succeeds in quantitatively modeling specific experimental data with neurobiologically-realistic timing parameters, and neither explains the relative reduction of STDP as the synaptic efficacy increases as we do. Nonetheless, these models make an interesting contrast to ours by suggesting a computational principle of optimization of information transmission, as contrasted

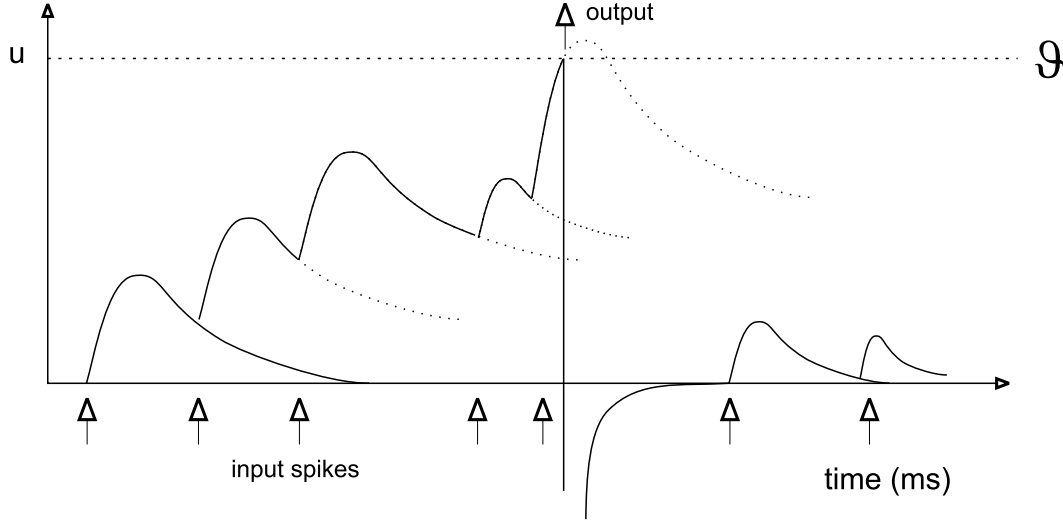


Figure 2: Membrane potential  $u(t)$  of a neuron as a sum of weighted excitatory PSP kernels due to impinging spikes. Arrival of PSP's marked by arrows; once the membrane potential reaches threshold it is reset and a reset function  $\eta$  is added to model the recovery effects of the threshold.

with our principle of neural noise reduction. Experimental tests might be devised to distinguish between these competing theories.

In Section 2 we describe the sSRM, and in Section 3 we derive the minimal entropy gradient. In Section 4 we describe the STDP experiment which we simulate in Section 5. We conclude with Section 6.

## 2. THE STOCHASTIC SPIKE RESPONSE MODEL

The Spike Response Model (SRM), defined by Gerstner (2001), is a generic integrate-and-fire model of a spiking neuron that closely corresponds to the behavior of a biological spiking neuron and is characterized in terms of a small set of easily interpretable parameters (Jolivet, Lewis, & Gerstner, 2003; Paninski, Pillow, & Simoncelli, 2005). The standard SRM formulation describes the temporal evolution of the membrane potential based on past neuronal events, specifically as a weighted sum of postsynaptic potentials (PSP's) modulated by reset and threshold effects of previous postsynaptic spiking events. The general idea is depicted in Figure 2; formally (following Gerstner, 2001), the membrane potential  $u_i(t)$  of cell  $i$  at time  $t$  is defined as:

$$u_i(t) = \sum_{f_i \in \mathcal{G}_i^t} \eta(t - f_i) + \sum_{j \in \Gamma_i} w_{ij} \sum_{f_j \in \mathcal{G}_j^t} \epsilon(t|f_j, \mathcal{G}_i^t), \quad (2.1)$$

where  $\Gamma_i$  is the set of inputs connected to neuron  $i$ ,  $\mathcal{G}_i^t$  is the set of times prior to  $t$  that a neuron  $i$  has spiked, with firing times  $f_i \in \mathcal{G}_i^t$ ;  $w_{ij}$  is the synaptic weight from neuron  $j$  to neuron  $i$ ,  $\epsilon(t|f_j, \mathcal{G}_i^t)$  is the PSP in neuron  $i$  due to an input spike from neuron  $j$  at time  $f_j$  given postsynaptic firing history  $\mathcal{G}_i^t$ , and  $\eta(t - f_i)$  is the refractory response due to the postsynaptic spike at time  $f_i$ .

To model the postsynaptic potential  $\epsilon$  in a leaky-integrate-and-fire neuron, a spike of presynaptic neuron  $j$  emitted at time  $f_j$  generates a postsynaptic current  $\alpha(t)$  for a presynaptic spike arriving at  $f_j$  for  $t > f_j$ . In the absence of postsynaptic firing this kernel (following Gerstner and Kistler (2002), Eqs (4.62)–(4.56), pp. 114–115) can be computed as:

$$\epsilon(t|f_j) = \int_{f_j}^t \exp\left(-\frac{s-f_j}{\tau_m}\right) \alpha(s-f_j) ds, \quad (2.2)$$

where  $\tau_m$  is the decay time of the postsynaptic neuron's membrane potential. Consider an exponentially decaying postsynaptic current  $\alpha(t)$  of the form

$$\alpha(t) = \frac{1}{\tau_s} \exp\left(-\frac{t}{\tau_s}\right) \mathcal{H}(t), \quad (2.3)$$

(Figure 3a), where  $\tau_s$  is the decay time of the current and  $\mathcal{H}(t)$  is the Heaviside function. In the absence of postsynaptic firing, this current contributes a postsynaptic potential of the form

$$\epsilon(t|f_j) = \frac{1}{1 - \tau_s/\tau_m} \left[ \exp\left(-\frac{(t-f_j)}{\tau_m}\right) - \exp\left(-\frac{(t-f_j)}{\tau_s}\right) \right] \mathcal{H}(t-f_j), \quad (2.4)$$

with current decay time-constant  $\tau_s$  and decay time-constant  $\tau_m$ .

When the postsynaptic neuron fires after the presynaptic spike arrives— at some time  $\hat{f}_i$  following presynaptic spike at time  $f_j$ — the membrane potential is reset, and only the remaining synaptic current  $\alpha(t')$  for  $t' > \hat{f}_i$  is integrated in Equation (2.2). Following Gerstner, 2001 (Section 4.4, Equation 1.66), the PSP that takes such postsynaptic firing into account can be written as

$$\epsilon(t|f_j, \hat{f}_i) = \begin{cases} \epsilon(t|f_j) & \hat{f}_i < f_j, \\ \exp\left(-\frac{(f_j-\hat{f}_i)}{\tau_s}\right) \epsilon(t|f_j) & \hat{f}_i \geq f_j. \end{cases} \quad (2.5)$$

This function is depicted in Figure 3b, for the cases when a postsynaptic spike occurs both before and after the presynaptic spike. In principle, this formulation can be expanded to include the postsynaptic neuron firing more than once after the onset of the postsynaptic potential. However, for fast current decay times  $\tau_s$ , it is only useful to consider the residual current input for the first postsynaptic spike after onset and assume that any further postsynaptic spiking is modeled by a postsynaptic potential reset to zero from that point on.

The reset response  $\eta(t)$  models two phenomena. First, a neuron can be in a refractory period: it simply cannot spike again for about a millisecond after a spiking event. Second, after the emission of a spike, the threshold of the neuron may initially be elevated and then recover to the original value (Kandel, Schwartz, & Jessell, 2000). The SRM models this behavior as negative contributions to the membrane potential (Equation 2.1): with  $s = t - \hat{f}_i$  denoting the time since the postsynaptic spike, the refractory reset function is defined as (Gerstner, 2001):

$$\eta(s) = \begin{cases} \mathcal{U}_{abs} & 0 < s < \delta_r \\ \mathcal{U}_{abs} \exp\left(-\frac{s+\delta_r}{\tau_r^f}\right) + \mathcal{U}_r \exp\left(-\frac{s}{\tau_r^s}\right) & s \geq \delta_r, \end{cases} \quad (2.6)$$

where a large negative impulse  $\mathcal{U}_{abs}$  models the absolute refractory period, with duration  $\delta_r$ ; the absolute refractory contribution smoothly resets via a fast decaying exponential with time constant  $\tau_r^f$ . The term  $\mathcal{U}_r$  models the slow exponential recovery of the elevated threshold with time constant  $\tau_r^s$ . The function  $\eta$  is depicted in Figure 3c.

We made a minor modification to the SRM described in (Gerstner, 2001) by relaxing the constraint that  $\tau_r^s = \tau_m$ , and also by smoothing the absolute refractory function (such smoothing is mentioned in Gerstner (2001) but is not explicitly defined). In all simulations, we use  $\delta_r = 1\text{ms}$ ,  $\tau_r^s = 3\text{ms}$ , and  $\tau_r^f = 0.25\text{ ms}$  (in line with estimates for biological neurones, Kandel et al. (2000), the smoothing parameter was chosen to be fast compared to  $\tau_r^s$ ).

The SRM we just described is deterministic. Gerstner (2001) introduces a stochastic variant of the SRM (*sSRM*) by incorporating the notion of a stochastic firing threshold: given membrane potential

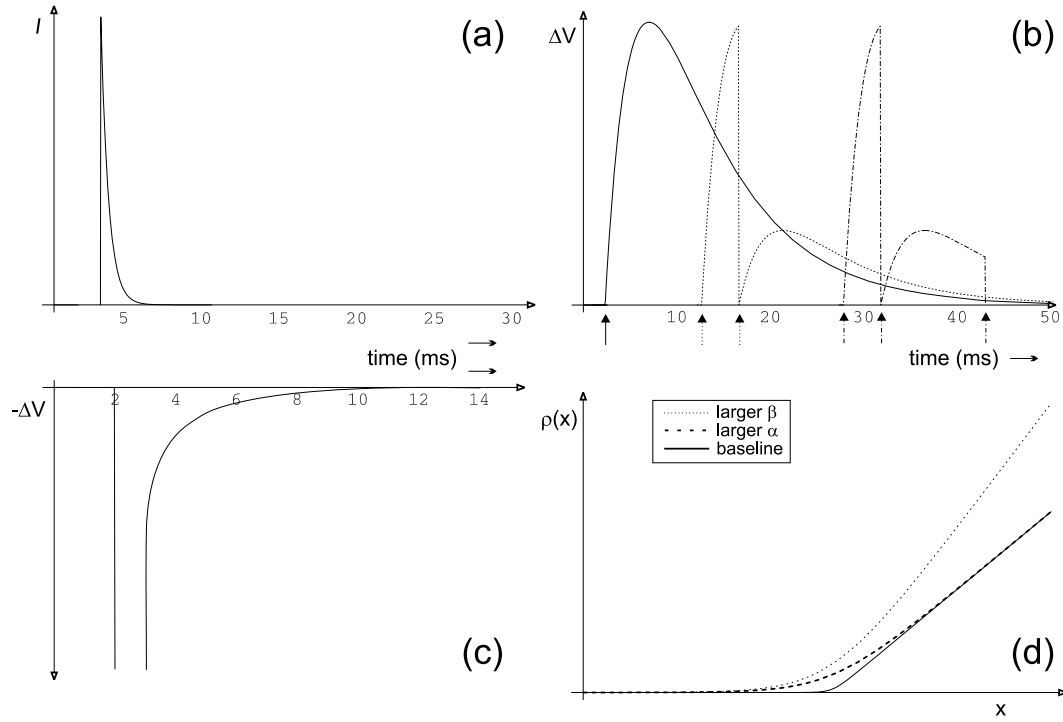


Figure 3: (a)  $\alpha(t)$  function: synaptic input modeled as exponentially decaying current. (b) Postsynaptic potential due to a synaptic input in the absence of postsynaptic firing (solid line), and with postsynaptic firing once and twice (dotted respectively dashed lines, postsynaptic spikes indicated by arrow) (c) reset function  $\eta(t)$ , (d) spike probability  $\rho(u)$  as a function of potential  $u$  for different values of  $\alpha$  and  $\beta$  parameters.



$u_i(t)$ , the probability of the neuron firing at time  $t$  is specified by  $\rho(u_i(t))$ . Herrmann and Gerstner (2001) find that for a reasonable escape-rate noise model of the integration of current in real neurons, the probability of firing is small and constant for small potentials, but around a threshold  $\vartheta$ , the probability increases linearly with the potential. In our simulations, we use such a function:

$$\rho(v) = \frac{\beta}{\alpha} \{ \ln[1 + \exp(\alpha(\vartheta - v))] - \alpha(\vartheta - v) \}, \quad (2.7)$$

where  $\alpha$  determines the abruptness of the constant-to-linear transition in the neighborhood of threshold  $\vartheta$ , and  $\beta$  determines the slope of the linear increase beyond  $\vartheta$ . This function is depicted in Figure 3d for several values of  $\alpha$  and  $\beta$ . We remark that we also conducted simulation experiments with sigmoidal and exponential density functions, and found no qualitative difference in the results.

### 3. MINIMIZING CONDITIONAL ENTROPY

We now derive the rule for adjusting the weight from a presynaptic input neuron  $j$  to a postsynaptic neuron  $i$ , so as to minimize the entropy of  $i$ 's response given a particular spike train from  $j$ .

A spike train is described by the set of all times at which a neuron  $i$  emitted spikes within some interval between 0 and  $T$ , denoted  $\mathcal{G}_i^T$ . We assume the interval is wide enough that the occurrence of spikes outside the interval do not influence the state of a neuron within the interval (e.g., through threshold reset effects). This assumption allows us to treat intervals as independent of each other. The set of input spikes received by neuron  $i$  during this interval is denoted  $\mathcal{F}_i^T$ , which is just the union of all output spike trains of connected presynaptic neurons  $j$ :  $\mathcal{F}_i^T = \bigcup \mathcal{G}_j^T \forall j \in \Gamma_i$ .

Given input spikes  $\mathcal{F}_i^T$ , the stochastic nature of neuron  $i$  may lead not only to the observed response  $\mathcal{G}_i^T$ , but a range of other possibilities. Denoting the set of possible responses  $\Omega_i$ , where  $\mathcal{G}_i^T \in \Omega_i$ . Further, let binary variable  $\sigma(t)$  denote the state of the neuron in the time interval  $[t, t + \Delta t)$ , where  $\sigma(t) = 1$  means the neuron spikes and  $\sigma(t) = 0$  means no spike. A response  $\xi \in \Omega_i$  is then equivalent to  $[\sigma(0), \sigma(\Delta t), \dots, \sigma(T)]$ .

Given a probability density  $g(\xi)$  over all possible responses  $\xi$ , the differential entropy of neuron  $i$ 's response conditional upon input  $\mathcal{F}_i^T$  is then defined as:

$$h(\Omega_i | \mathcal{F}_i^T) = - \int_{\Omega_i} g(\xi) \log(g(\xi)) d\xi. \quad (3.1)$$

According to our hypothesis, a neuron adjusts its weights so as to minimize the conditional differential entropy. Such an adjustment is obtained by performing gradient descent on the conditional entropy with respect to the weights:

$$\Delta w_{ij} \propto - \frac{\partial h(\Omega_i | \mathcal{F}_i^T)}{\partial w_{ij}}. \quad (3.2)$$

In this section, we compute the right hand side of Equation (3.2) for an sSRM neuron. Substituting the entropy definition of Equation (3.1) into Equation (3.2), we obtain:

$$\begin{aligned} \frac{\partial h(\Omega_i | \mathcal{F}_i^T)}{\partial w_{ij}} &= - \frac{\partial}{\partial w_{ij}} \int_{\Omega} g(\xi) \log(g(\xi)) d\xi \\ &= - \int_{\Omega_i} g(\xi) \frac{\partial \log(g(\xi))}{\partial w_{ij}} (\log(g(\xi)) + 1) d\xi. \end{aligned} \quad (3.3)$$

We follow Xie and Seung (2004) to derive  $\frac{\partial \log(g(\xi))}{\partial w_{ij}}$  for a differentiable neuron model firing at times  $\mathcal{G}_i^T$ . First, note that  $g(\xi)$  can be factorized:

$$g(\xi) = \prod_{t=0}^T P(\sigma(t) | \{\sigma(t'), \forall t' < t\}), \quad (3.4)$$



because the states  $\sigma(t)$  are conditionally independent, and hence the factored probability  $P(\sigma(t)|\{\sigma(t')\})$  in the limit for small  $\Delta t$  is equivalent to the spike probability density of the membrane potential,  $\rho(u_i(t))$ . (For brevity, we write  $\rho_i(t)$  as shorthand for  $\rho(u_i(t))$ ). Noting further that:

$$\frac{\partial \ln(g(\xi))}{\partial w_{ij}} \equiv \frac{1}{g(\xi)} \frac{\partial g(\xi)}{\partial w_{ij}}$$

and

$$\frac{\partial \rho_i(t)}{\partial w_{ij}} = \frac{\partial \rho_i(t)}{\partial u_i(t)} \frac{\partial u_i(t)}{\partial w_{ij}}, \quad (3.6)$$

it is straightforward to derive:

$$\begin{aligned} \frac{\partial \log(g(\xi))}{\partial w_{ij}} &= \int_{t=0}^T \frac{\partial \rho_i(t)}{\partial u_i(t)} \frac{\partial u_i(t)}{\partial w_{ij}} \frac{\left( \sum_{f_i \in \mathcal{F}_i^T} \delta(t - f_i) - \rho_i(t) \right)}{\rho_i(t)} dt, \\ &= - \int_{t=0}^T \rho'_i(t) \epsilon(t|f_j, f_i) dt + \sum_{f_i \in \mathcal{F}_i^T} \frac{\rho'_i(f_i)}{\rho_i(f_i)} \epsilon(f_i|f_j, f_i), \end{aligned} \quad (3.7)$$

where  $\rho'_i(t) \equiv \frac{\partial \rho_i(t)}{\partial u_i(t)}$  and  $\delta(t - f_i)$  is the Dirac delta, and we use that in the sSRM formulation,

$$\frac{\partial u_i(t)}{\partial w_{ij}} = \epsilon(t|f_j, f_i).$$

The term  $\rho'_i(t)$  in Equation (3.7) can be computed for any differentiable spike probability function. In the case of Equation (2.7),

$$\rho'_i(t) = \frac{\beta}{1 + \exp(\alpha(\vartheta - u_i(t)))}.$$

Substituting our model for  $\rho_i(t)$ ,  $\rho'_i(t)$  from Equation (2.7) into Equation (3.7), we obtain

$$\begin{aligned} \frac{\partial \log(g(\xi))}{\partial w_{ij}} &= -\beta \int_{t=0}^T \frac{\epsilon(t|f_j, f_i)}{1 + \exp[\alpha(\vartheta - u_i(t))]} dt + \\ &+ \sum_{f_i \in \mathcal{G}_i^T} \frac{\epsilon(f_i|f_j, f_i)}{\alpha \left\{ \ln(1 + \exp[\alpha(\vartheta - u_i(f_i))]) - \alpha(\vartheta - u_i(f_i)) \right\} (1 + \exp[\alpha(\vartheta - u_i(f_i))])}. \end{aligned} \quad (3.8)$$

Equation (3.8) can be substituted into Equation (3.3), which when integrated provides the gradient-descent weight update that implements conditional entropy minimization (Equation (3.2)).

The hypothesis under exploration is that this gradient-descent weight update yields STDP. Unfortunately, an analytic solution to Equation (3.3) (and hence Equation (3.2)) is not readily obtained. Nonetheless, numerical methods can be used to obtain a solution.

We are not suggesting a neuron performs numerical integration of this sort in real time. It would be preposterous to claim biological realism for an instantaneous integration over all possible responses  $\xi \in \Omega_i$ , as specified by Equation (3.3). Consequently, we have a dilemma: What use is a computational theory of STDP if the theory demands intensive computations that could not possibly be performed by a neuron in real time? This dilemma can be circumvented in two ways. First, the resulting learning rule might be cached in some form through evolution so that the computation is not necessary. That is, the solution—the STDP curve itself—may be built into a neuron. As such, our computational theory provides an argument for why neurons have evolved to implement the STDP learning rule. Second, the specific response produced by a neuron on a single trial might be considered to be a sample from the distribution  $g(\xi)$ , and the integration in Equation (3.3) can be performed by a sampling process over repeated trials; each trial would produce a stochastic gradient step.

### 3.1 Numerical Computation

In this section, we describe the procedure for numerically evaluating Equation (3.2) via Simpson's integration (Hennion, 1962).

This integration is performed over the set of possible responses  $\Omega_i$  (Equation (3.3)) within the time interval  $[0 \dots T]$ . The set  $\Omega_i$  can be divided into disjoint subsets  $\Omega_i^n$  which contain **exactly  $n$  spikes**:  $\Omega_i = \bigcup \Omega_i^n \forall n$ .

Using this breakdown,

$$\begin{aligned} \frac{\partial h(\Omega_i | \mathcal{F}_i^T)}{\partial w_{ij}} &= - \int_{\Omega_i} g(\xi) (\log(g(\xi)) + 1) \frac{\partial \log(g(\xi))}{\partial w_{ij}} d\xi, \\ &= - \sum_{n=0}^{\infty} \int_{\Omega_i^n} g(\xi) (\log(g(\xi)) + 1) \frac{\partial \log(g(\xi))}{\partial w_{ij}} d\xi. \end{aligned} \quad (3.10)$$

In the experimental conditions that we model, the probability of  $n > 2$  spikes is vanishingly small. (We have verified this claim by computing the probability of  $n \leq 2$  and only using those simulation parameters where this probability is larger than 0.999). Thus, we need only compute Equation (3.10) for  $n \in 0, 1, 2$ .

It is illustrative to walk through the alternatives. For  $n = 0$ , there is only one response given the input. Assuming the probability of  $n = 0$  spikes is  $p_0$ , the  $n = 0$  term of Equation (3.10) reads:

$$\frac{\partial h(\Omega_i | \mathcal{F}_i^T)}{\partial w_{ij}} = p_0 (\log(p_0) + 1) \int_{t=0}^T -\rho'_i(t) \epsilon(t | f_j, f_i) dt. \quad (3.11)$$

The probability  $p_0$  is the probability of the neuron not having fired between  $t = 0$  and  $t = T$  given inputs  $\mathcal{F}_i^T$  resulting in membrane potential  $u_i(t)$  and hence probability of firing at time  $t$  of  $\rho(u_i(t))$ :

$$p_0 = S[0, T] = \exp\left(- \int_{t=0}^T \rho(u_i(t)) dt\right), \quad (3.12)$$

which is equal to the survival function  $S$  for a non-homogenous Poisson process with probability density  $\rho(u_i(t))$  for  $t = [0 \dots T]$ . (We use the inclusive/exclusive notation for  $S$ :  $S(0, T)$  computes the function excluding the endpoints,  $S[0, T]$  is inclusive.)

For  $n = 1$ , we must consider all responses containing exactly one output spike:  $\mathcal{G}_i^T = \{f_i^1\}$ ,  $f_i^1 \in [0, T]$ . Assuming that neuron  $i$  fires only at time  $f_i^1$  with probability  $p_1(f_i^1)$ , the  $n = 1$  term of Equation (3.10) reads:

$$\begin{aligned} \frac{\partial h(\Omega_i | \mathcal{F}_i^T)}{\partial w_{ij}} &= \int_{f_i^1=0}^{f_i^1=T} p_1(f_i^1) (\log(p_1(f_i^1)) + 1) \left[ \int_{t=0}^T -\rho'_i(t) \epsilon(t | f_j, f_i^1) dt + \right. \\ &\quad \left. + \frac{\rho'_i(f_i^1)}{\rho_i(f_i^1)} \epsilon(f_i^1 | f_j, f_i^1) \right] df_i^1. \end{aligned} \quad (3.14)$$

The probability  $p_1(f_i^1)$  is computed as:

$$p_1(f_i^1) = S[0, f_i^1] \rho_i(f_i^1) S(f_i^1, T], \quad (3.15)$$

where the membrane potential now incorporates one reset at  $t = f_i^1$ :

$$u_i(t) = \eta(t - f_i^1) + \sum_{j \in \Gamma_i} w_{ij} \sum_{f_j \in \mathcal{F}_j^t} \epsilon(t | f_j, f_i^1)$$

For  $n = 2$ , we must consider all responses containing exactly two output spikes:  $\mathcal{G}_i^T = \{f_i^1, f_i^2\}$  for  $f_i^1, f_i^2 \in [0, T]$ . Assuming that neuron  $i$  fires at  $f_i^1$  and  $f_i^2$  with probability  $p_2(f_i^1, f_i^2)$ , the

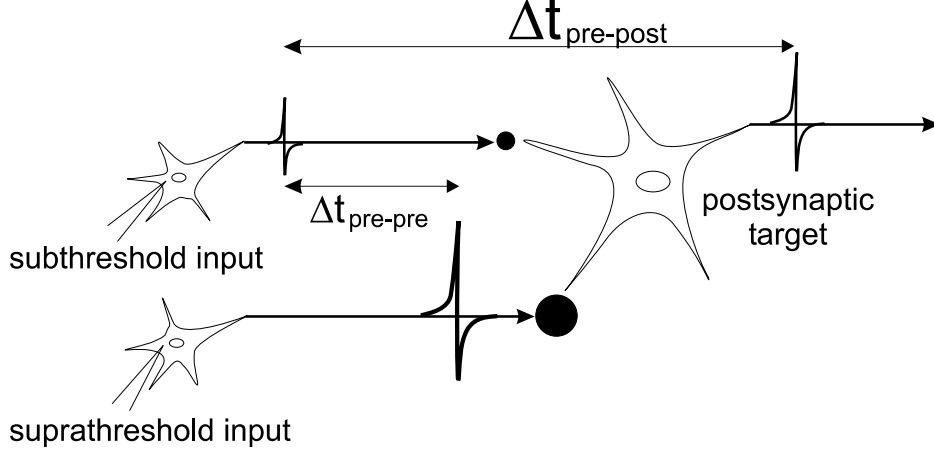


Figure 4: Experimental setup of Zhang et al. (1998)

$n = 2$  term of Equation (3.10) reads:

$$\begin{aligned} \frac{\partial h(\Omega_i | \mathcal{F}_i^T)}{\partial w_{ij}} &= \int_{f_i^1=0}^{f_i^1=T} \int_{f_i^2=f_i^1}^{f_i^2=T} p_2(f_i^1, f_i^2) \left( \log(p_2(f_i^1, f_i^2)) + 1 \right) \left[ \int_{t=0}^T -\rho'_i(t) \epsilon(t | f_j, f_i^1, f_i^2) dt + \right. \\ &\quad \left. + \frac{\rho'_i(f_i^1)}{\rho_i(f_i^1)} \epsilon(f_i^1 | f_j, f_i^1, f_i^2) + \frac{\rho'_i(f_i^2)}{\rho_i(f_i^2)} \epsilon(f_i^2 | f_j, f_i^1, f_i^2) \right] df_i^1 df_i^2. \end{aligned} \quad (3.16)$$

The probability  $p_2(f_i^1, f_i^2)$  can again be expressed in terms of the survival function:

$$p_2(f_i^1, f_i^2) = S[0, f_i^1] \rho_i(f_i^1) S[f_i^1, f_i^2] \rho_i(f_i^2) S(f_i^2, T), \quad (3.17)$$

with  $u_i(t) = \eta(t - f_i^1) + \eta(t - f_i^2) + \sum_{j \in \Gamma_i} w_{ij} \sum_{f_j \in \mathcal{F}_j^t} \epsilon(t | f_j, f_i^1, f_i^2)$ .

In this section, we have replaced an integral over possible spike sequences  $\Omega_i$  with an integral over the time of two output spikes,  $f_i^1$  and  $f_i^2$ , which we compute numerically.

#### 4. SIMULATION METHODOLOGY

We modeled in detail the [experiment of Zhang et al. \(1998\)](#) involving asynchronous co-stimulation of convergent inputs. In this experiment, depicted in Figure 4, a *postsynaptic* neuron is identified that has two neurons projecting to it, [one weak \(subthreshold\)](#) and [one strong \(suprathreshold\)](#). The subthreshold input results in depolarization of the postsynaptic neuron, but the depolarization is not strong enough to cause the postsynaptic neuron to spike. The suprathreshold input is strong enough to induce a spike in the postsynaptic neuron. Plasticity of the synapse between the subthreshold input and the postsynaptic neuron is measured as a function of the timing between subthreshold and postsynaptic neurons' spikes ( $\Delta t_{pre-post}$ ) by varying the intervals between induced spikes in the subthreshold and the suprathreshold inputs ( $\Delta t_{pre-pre}$ ). This measurement yields the well-known STDP curve (Figure 1b).

In most experimental studies of STDP, the postsynaptic neuron is induced to spike not via a suprathreshold neuron, [but rather by depolarizing current injection directly into the postsynaptic neuron](#). To model experiments that induce spiking via current injection, additional assumptions must be made in the Spike Response Model framework. Because these assumptions are not well established in the literature, we have focused on the synaptic input technique of Zhang et al. (1998). In Section 5.1, we propose a method for modeling a depolarizing current injection in the spike-response model.

The Zhang et al. (1998) experiment imposes **four constraints on a simulation**. (1) The suprathreshold input alone causes spiking  $> 70\%$  of the time. (2) The subthreshold input alone causes spiking  $< 10\%$  of the time. (3) Synchronous firing of suprathreshold and/or subthreshold inputs cause LTP if and only if the postsynaptic neuron fires. (4) The time constants of the excitatory PSPs (EPSPs) — $\tau_s$  and  $\tau_m$  in the sSRM—are in the range of 1–5ms and 7–15ms respectively. These constraints remove many free parameters from our simulation. We do not explicitly model the two input cells; instead, we **model the EPSPs** they produce. The magnitude of these EPSPs are picked to satisfy the experimental constraints: in most simulations, unless reported otherwise, the suprathreshold EPSP alone causes a spike in the post on 85% of trials, and the subthreshold EPSP alone causes a spike on fewer than 0.1% of trials. Free parameters of the simulation are  $\vartheta$  and  $\beta$  in the spike-probability function ( $\alpha$  can be folded into  $\vartheta$ ), and the magnitude ( $u_r^s, u_{abs}$ ) and time constants ( $\tau_r^s, \tau_r^f, \Delta_{abs}$ ) of the reset. We can further investigate how the results depend on the exact strengths of the subthreshold and suprathreshold EPSP's.

The dependent variable of the simulation is  $\Delta t_{pre-post}$ , and we measure the time of the post spike to determine  $\Delta t_{pre-post}$ . We estimate the weight update for a given  $\Delta t_{pre-post}$  using Equation 3.2 by approximating the integral by a summation over all time-discretized output responses consisting of 0, 1, or 2 spikes (see Section 3.1). Three or more spikes have a probability that is vanishingly small ( $p < 0.001$ ).

## 5. RESULTS

Figure 5 shows an STDP curve produced by the model, obtained by plotting the estimated weight update of Equation (3.2) against  $\Delta t_{pre-post}$ . Specifically, we vary the difference in time between subthreshold and suprathreshold inputs (**a pre-pre pair**). For each pre-pre pair, we compute the expected gradient over all responses of the postsynaptic neuron via Equation (3.2), obtaining in a value for  $\Delta w$  for each  $\Delta t_{pre-pre}$  data point. The corresponding value  $\Delta t_{pre-post}$  is determined by calculating for each input pair the average time at which the postsynaptic neuron fires relative to the subthreshold input. Together, this results in a set of  $(\Delta t_{pre-post}, \Delta w)$  data points. The continuous graph is obtained by connecting these points. By our assumption that the weight update is proportional to the gradient computed in Equation (3.2), the simulation curve is globally scaled to match the neurophysiological results. For this reason, the units on the y-axis of Figure 5 are arbitrary.

The model produces an excellent fit to the experimental data points (triangles), and robustly obtains **the typical LTP/LTD time windows associated with STDP**. The qualitative shape of the STDP curve is robust to settings of the spiking neuron model's parameters, as we will illustrate shortly. Additionally, we found that the type of spike-probability function  $\rho$  (**exponential, sigmoidal, or linear**) is not critical.

Our model accounts for an additional finding that has not been explained by alternative theories: **The relative magnitude of LTP decreases as the efficacy of the synapse between the subthreshold input and the postsynaptic target neuron increases**; in contrast, LTD remains roughly constant (G.-q. Bi & Poo, 1998), Figure 6a shows this effect in the experiment of Bi and Poo (1998), and Figure 6b shows the corresponding result from our model. We compute the magnitude of LTP and LTD for the peak modulation (i.e.,  $\Delta t_{pre-post} = -5$  for LTP and  $\Delta t_{pre-post} = +5$  for LTD) as the amplitude of the subthreshold EPSP is increased. The model's explanation for this phenomenon is simple: **As the synaptic weight increases, its effect saturates, and a small change to the weight does little to alter its influence**. Consequently, the gradient of the entropy with respect to the weight goes toward zero. Similar saturation effects are observed in gradient-based learning methods with nonlinear response functions, such as back propagation.

As we mentioned earlier, other theories have had difficulty reproducing the LTD component of STDP. This component arises in our model due to noise in the neural response: suppression is needed to prevent multiple spikes. To argue for this conclusion, we performed simulations that make our neuron model less noisy in various ways, and each of these manipulations results in a reduction in the LTD component of STDP. In Figures 7a and 7b, we make the threshold more deterministic by increasing the values of  $\alpha$  and  $\beta$  in the spike probability density function. In Figure 7c, we increase the

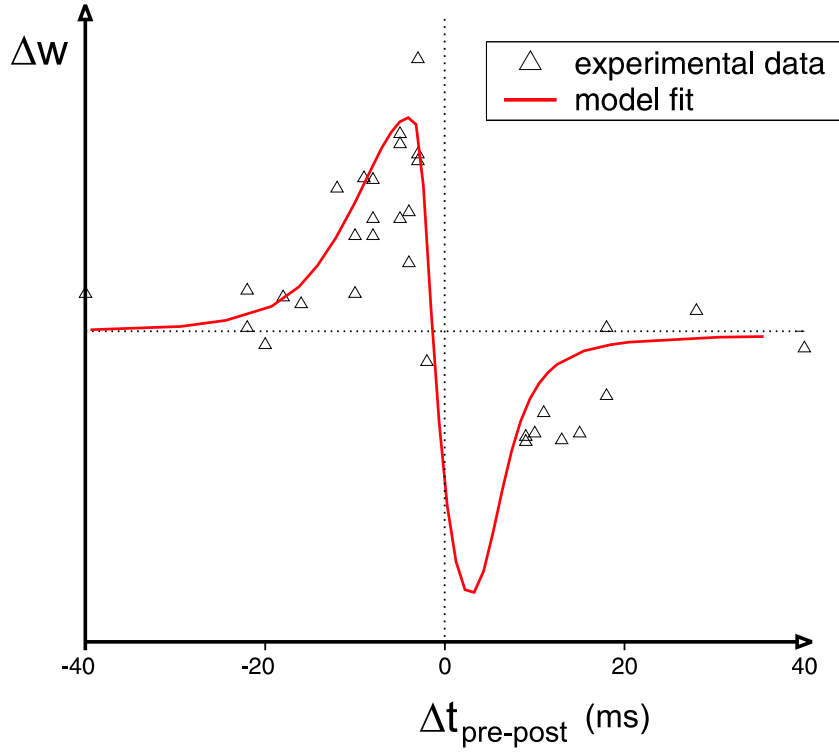


Figure 5: STDP – experimental data (triangles) and model fit (solid line). STDP data redrawn from Zhang et al. (1998). Model parameters:  $\tau_s = 2.5\text{ms}$ ,  $\tau_m = 10\text{ms}$ .

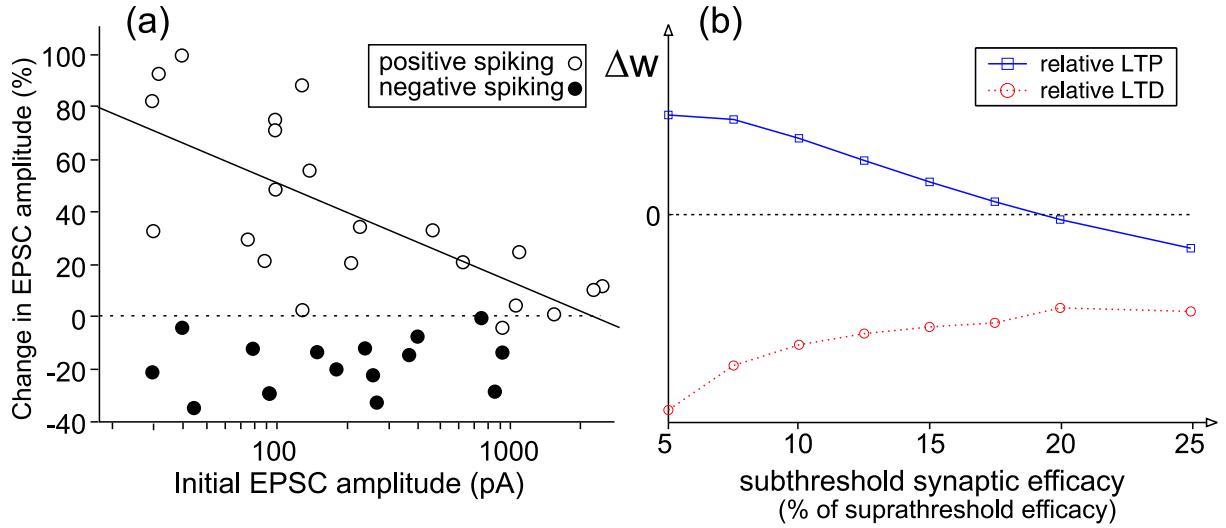


Figure 6: Dependence of LTP and LTD magnitude on efficacy of the subthreshold input. (a) Experimental data redrawn from Bi & Poo (1998); (b) Simulation result.

magnitude of the refractory response  $\eta$ , which will prevent spikes following the initial postsynaptic response. And finally, in Figure 7d, we increase the efficacy of the suprathreshold input, which

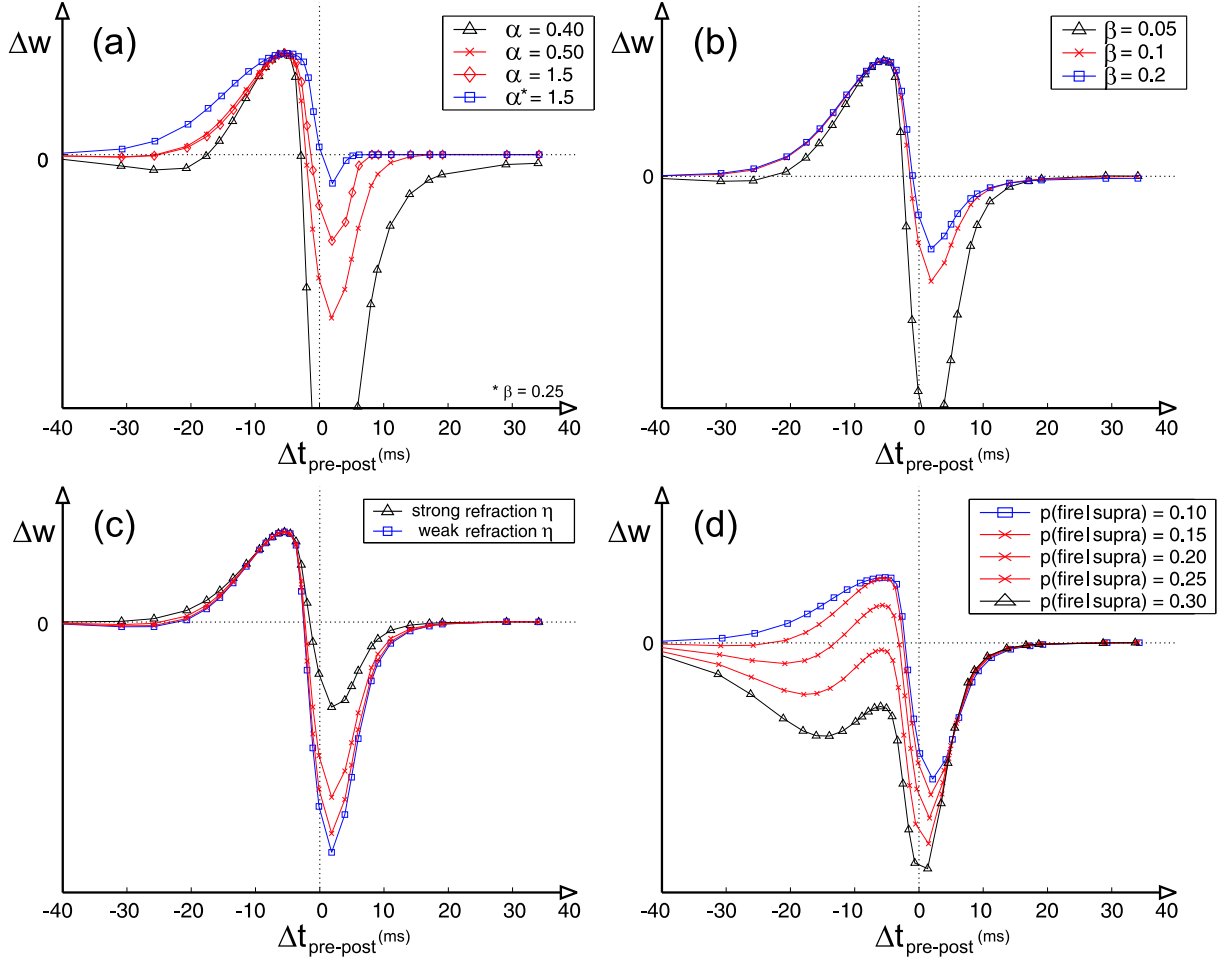


Figure 7: Dependence of relative LTP and LTD on (a) the parameter  $\alpha$  of the stochastic threshold function, (b) the parameter  $\beta$  of the stochastic threshold function, (c) the magnitude of refraction,  $\eta$ , and (d) efficacy of the suprathreshold synapse, expressed as  $p(\text{fire}|\text{supra})$ , the probability that the postsynaptic neuron will fire when receiving only the suprathreshold input. Larger values of  $p(\text{fire}|\text{supra})$  correspond to a weaker suprathreshold synapse. In all graphs, the weight gradient for individual curves is normalized to peak LTP for comparison purposes.

prevents the postsynaptic neuron's potential from hovering in the region where noise can induce a spike. Modulation of all of these variables make the threshold more deterministic, and decrease LTD relative to LTP.

Our simulation results are robust to biologically-realizable variation in the parameters of the sSRM model. For example, time constants of the EPSPs can be varied with no qualitative effect on the STDP curves. Figures 8a and 8b show the effect of manipulating the membrane potential decay time  $\tau_m$  and the EPSP rise time  $\tau_s$ , respectively. Note that manipulation of these time constants does predict a systematic effect on STDP curves. Increasing  $\tau_m$  increases the duration of both the LTP and LTD windows, whereas decreasing  $\tau_s$  leads to a faster transition from LTP to LTD. Both predictions could be tested experimentally by correlating time constants of individual neurons studied with the time course of their STDP curves.

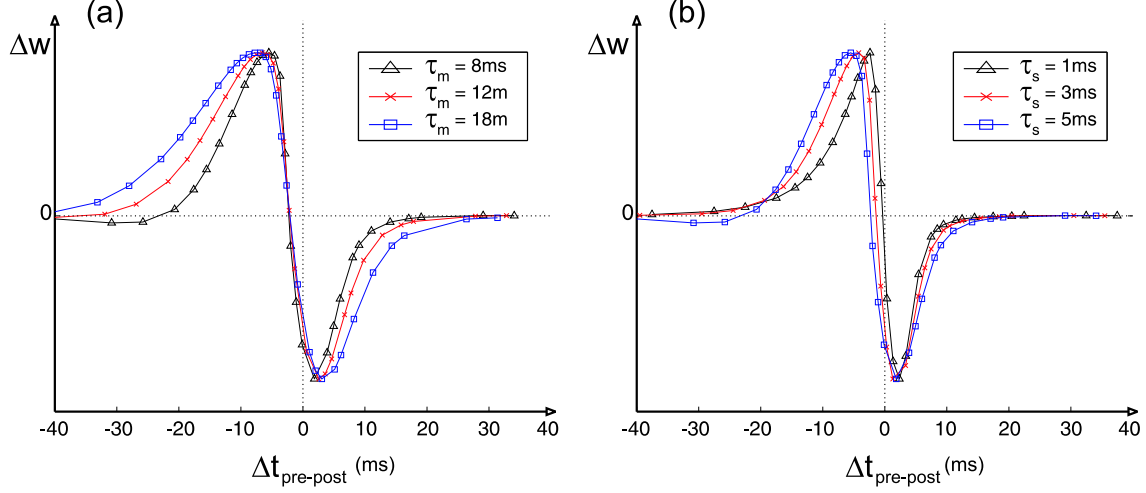


Figure 8: Influence of time constants of the sSRM model on the shape of the STDP curve. (a) varying the membrane potential time-constant  $\tau_m$  (b) varying the EPSP rise time constant  $\tau_s$ . In both figures, the magnitude of LTP and LTD have been normalized to 1 for each curve to allow for easy examination of the effect of the manipulation on temporal characteristics of the STDP curves.

### 5.1 Current Injection

We mentioned earlier that in many STDP experiments, an action potential is induced in the postsynaptic neuron not via a suprathreshold presynaptic input, but via a depolarizing current injection. In order to model experiments using current injection, we must characterize the current function and its effect on the postsynaptic neuron. In this section, we make such a proposal framed in terms of the Spike Response Model, and report simulation results using current injection.

We model the injected current  $\mathcal{I}(t)$  as a rectangular step function:

$$\mathcal{I}(t) = \mathcal{H}(t - f_I) \mathcal{I}_c \mathcal{H}(t - [f_I + \Delta_I]), \quad (5.1)$$

where the current of magnitude  $\mathcal{I}_c$  is switched on at  $t = f_I$  and off at  $t = f_I + \Delta_I$ . In the Zhang et al (1998) experiment,  $\Delta_I$  is 2ms, a value we adopted for our simulations as well.

The resulting postsynaptic potential,  $\epsilon_c$  is:

$$\epsilon_c(t) = \int_0^t \exp\left(-\frac{s}{\tau_m}\right) \mathcal{I}(s) ds. \quad (5.2)$$

In the absence of postsynaptic firing, the membrane potential of an integrate-and-fire neuron in response to a step current is (Gerstner, 2001):

$$\epsilon_c(t|f_I) = \mathcal{I}_c(1 - \exp[-(t - f_I)/\tau_m]). \quad (5.3)$$

In the presence of postsynaptic firing at time  $\hat{f}_i$ , we assume—as we did previously in Equation (2.5)—a reset and subsequent integration of the residual current:

$$\begin{aligned} \epsilon_c(t|\hat{f}_i) &= \mathcal{H}(\hat{f}_i - t) \int_0^t \exp\left(-\frac{s}{\tau_m}\right) \mathcal{I}(s) ds + \\ &\quad \mathcal{H}(t - \hat{f}_i) \int_{\hat{f}_i}^t \exp\left(-\frac{s}{\tau_m}\right) \mathcal{I}(s) ds. \end{aligned} \quad (5.4)$$



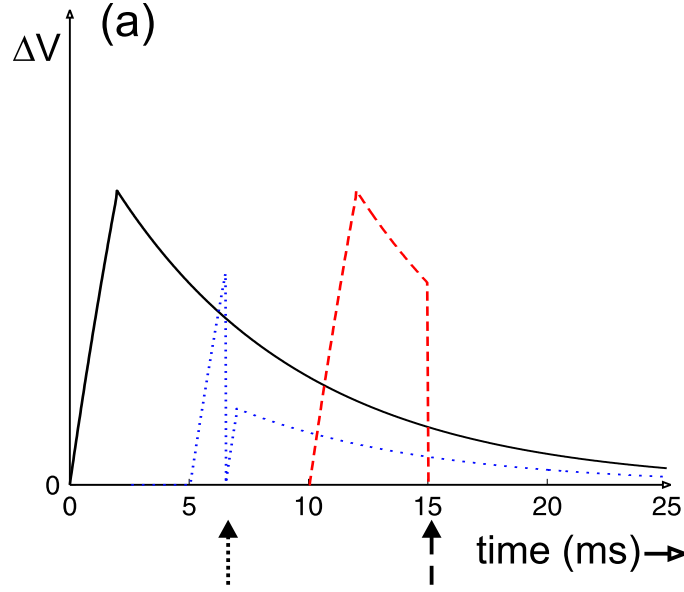


Figure 9: Voltage response of a spiking neuron for a 2ms current injection in the Spike Response Model. Solid curve: The postsynaptic neuron produces no spike, and the potential due to the injected current decays with the membrane time-constant  $\tau_m$ . Dotted curve: The postsynaptic neuron spikes while the current is still being applied. Dashed curve: The postsynaptic neuron spikes after application of the current has terminated (moment of postsynaptic spiking indicated by arrows).

These  $\epsilon_c$  kernels are depicted in Figure 9 for a postsynaptic spike occurring at various times  $\hat{f}_i$ . In our simulations, we chose the current magnitude  $\mathcal{I}_c$  to be large enough to elicit spiking of the target neuron with probability greater than 0.7.

Figure 10a shows the STDP curve obtained using the current injection model for the exact same model parameter settings used to produce the result based on a suprathreshold synaptic input (depicted in Figure 5) superimposed on the experimental data STDP obtained by depolarizing current injection from Zhang et al (1998). Figure 10b additionally superimposes the earlier result on the current injection result, and the two curves are difficult to distinguish. As in the earlier result, variation of model parameters has little appreciable effect on the model’s behavior using the current injection paradigm, suggesting that current injection vs. synaptic input makes little difference on the nature of STDP.

## 6. DISCUSSION

In this paper, we explored a fundamental computational principle, that synapses adapt so as to **minimize the variability of a neuron’s response in the face of noisy inputs**, yielding more reliable neural representations. From this principle—instantiated as entropy minimization—we derived the STDP learning curve. Importantly, the simulation methodology we used to derive the curve closely follows the procedure used in neurophysiological experiments (Zhang et al., 1998). Our simulations obtain an STDP curve that is robust to model parameters and details of the noise distribution.

Our results are critically dependent on the use of Gerstner’s stochastic Spike Response Model, whose dynamics are a good approximation to those of a biological spiking neuron. The sSRM has the virtue of being characterized by parameters that are readily related to neural dynamics, and its dynamics are differentiable such that we can derive a gradient-descent learning rule that minimizes the response variability of a postsynaptic neuron given a particular set of input spikes.

Our model predicts the shape of the STDP curve and how it relates to properties of a neuron’s

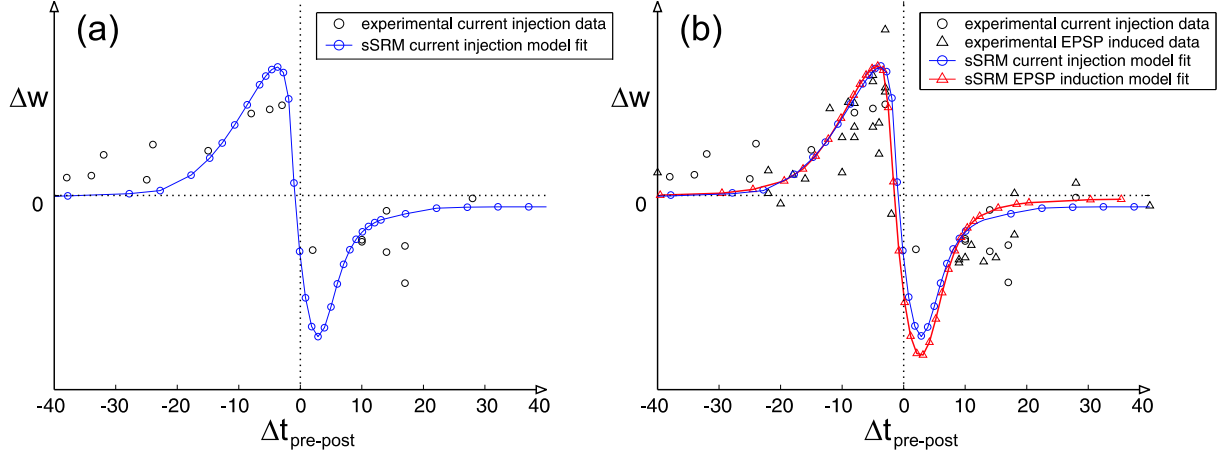


Figure 10: (a) STDP curve obtained for SRM with current injection (curve with solid circles) compared with experimental data for depolarizing current injection (redrawn from Zhang et al., (1998)). (b) Comparing STDP curves for both current injection (curve with circles) and suprathreshold input (curve with triangles) models. The same model parameters are used for both curves. Experimental data redrawn from Zhang et al. (1998) for current injection (circles) and suprathreshold input (triangles) paradigms are superimposed.

response function. These predictions may be empirically testable if a diverse population of cells can be studied. The predictions include the following: First, The width of the LTP and LTD windows depend on the (excitatory) PSP time constants (Figure 7a,b). Second, the strength of LTD relative to LTP depends on the degree of noise in the neuron’s response; the LTD strength is related to the noise level.

Our model also can characterize the nature of the learning curve for experimental situations that deviate from the boundary conditions of Zhang et al. (1998). In Zhang et al., the subthreshold and suprathreshold inputs produced postsynaptic firing with probability less than .10 and greater than .70, respectively. Our model can predict the consequences of violating these conditions. For example, when the subthreshold input is very strong or the suprathreshold input is very weak, our model produces strictly LTD, i.e., anti-Hebbian learning. The consequence of a strong subthreshold input is shown in Figure 6b, and the consequence of a weak suprathreshold input is shown in Figure 7d. Intuitively, this simulation result makes sense because—in the first case—the most likely alternative response of the postsynaptic neuron is to produce more than one spike, and—in the second case—the most likely alternative response is no postsynaptic spike at all. In both cases, synaptic depression reduces the probability of the alternative response. We note that such strictly anti-Hebbian learning has been reported in relation to STDP-type experiments (Roberts & Bell, 2002).

For very noisy thresholds and for weak suprathreshold inputs, our model produces an LTD “dip” before LTP (Figure 7d). We find it intriguing that this dip is also observed in the experimental results of Nishiyama et al. (2000). With careful consideration of experimental conditions and neuron parameters, it may be possible to reconcile the somewhat discrepant STDP curves obtained in the literature via our model.

In our model, the transition from LTP to LTD occurs at a slight offset from  $\Delta t_{\text{pre-post}} = 0$ : if the subthreshold input fires 1–2ms before the postsynaptic neuron fires (on average), then neither potentiation nor depression occurs. This 1–2ms offset is attributable to the current decay time constant,  $\tau_s$ . The neurophysiological data are not sufficiently precise to determine the exact offset of the LTP/LTD transition in real neurons. Unfortunately, few experimental data points are recorded near  $\Delta t_{\text{pre-post}} = 0$ . However, the STDP curve of our model does pass through the one data point in that

region (Figure 5), so the offset may actually be a real phenomenon.

The main focus of the simulations in this paper was to replicate the experimental paradigm of Zhang et al. (1998), in which a suprathreshold presynaptic neuron is used to induce the postsynaptic neuron to fire. The Zhang et al. (1998) study is exceptional in that most other experimental studies of STDP use a depolarizing current injection to induce the postsynaptic neuron to fire. We are not aware of any established model for current injection within the SRM framework. We therefore proposed a model of current injection within the SRM framework in Section 5.1. The proposed model is an ideal abstraction of current injection that does not take into account effects like current onset and offset fluctuations inherent to such experimental methods. Even with these limitations in mind, the current injection model produced STDP curves very similar to the ones obtained by the simulation of the suprathreshold input induced postsynaptic firing.

The simulations reported in this paper account for classical STDP experiments in which a single presynaptic spike is paired with a single postsynaptic spike. The same methodology can be applied to model experimental paradigms involving multiple presynaptic and/or postsynaptic spikes. However, the computation involved becomes nontrivial. We are currently engaged in modeling data from the multi-spike experiments of Froemke and Dan (2002).

To close, we note that one set of simulation results we reported is particularly pertinent for comparing and contrasting our model to the related models of Toyozumi et al. (2005) and Bell and Parra (2005). The simulations reported in Figure 7 suggest that noise in our model is critical for obtaining the LTD component of STDP, and that parameters that reduce noise in the neural response also reduce LTD. First, we found that increasing the strength of neuronal refraction reduces noise and therefore diminishes the LTD component of STDP. In sharp contrast, Toyozumi et al. (2005) suggest that neuronal refraction is responsible for LTD. Because the two models are quite similar, it seems unlikely that the models make opposite predictions and the discrepancy may be due to Toyozumi et al. (2005)’s focus on analytical approximations to solve the mathematical problem at hand, limiting the validity of comparisons between that model and biological experiments in the process. Second, we found that altering parameters of the response threshold that cause the neuron to be more deterministic also reduce LTD in our derivation. Strikingly, Bell and Parra (2005) use a deterministic SRM neuron, and are unable to model the LTD component of STDP. Because noise suppression should be one consideration of a learning rule that adapts synapses so as to maximize mutual information between input and output—even if only implicitly—we hypothesize that modeling a stochastic threshold is key to obtaining LTD in Bell and Parra (2005). One key difference between our model and those of Toyozumi et al. (2005) and Bell and Parra (2005) is the hypothesized computational objective of a neuron. We hypothesize reduction of neural response variability whereas the other models hypothesize mutual information maximization. These two hypotheses should have sufficiently distinct implications that further empirical studies may garner support for one hypothesis or the other.

*Acknowledgement* Work of SMB supported by the Netherlands Organization for Scientific Research (NWO), TALENT grant S-62 588. The authors thank Gary Cottrell for insightful comments and encouragement.

## Bibliography

- Abbott, L., & Gerstner, W. (2004). Homeostasis and learning through spike-timing dependent plasticity. In D. Hansel, C. Chow, B. Gutkin, & C. Meunier (Eds.), *Methods and models in neurophysics*.
- Bel1, C. C., Han, V. Z., Sugawara, Y., & Grant, K. (1997). Synaptic plasticity in a cerebellum-like structure depends on temporal order. *Nature*, *387*, 278–281.
- Bell, A., & Parra, L. (2005). Maximising information yields spike timing dependent plasticity. In *Advances in neural information processing systems 17*. MIT Press.
- Bi, G.-Q. (2002, Dec). Spatiotemporal specificity of synaptic plasticity: cellular rules and mechanisms. *Biol. Cybern.*, *87*, 319–332.
- Bi, G.-q., & Poo, M.-m. (1998). Synaptic modifications in cultured hippocampal neurons: Dependence on spike timing, synaptic strength, and postsynaptic cell type. *J. Neurosci.*, *18*(24), 10464–10472.
- Bi, G.-q., & Poo, M.-m. (2001). Synaptic modification by correlated activity: Hebb’s postulate revisited. *Ann. Rev. Neurosci.*, *24*, 139–166.
- Burkitt, A., Meffin, H., & Grayden, D. (2004). Spike timing-dependent plasticity: The relationship to rate-based learning for models with weight dynamics determined by a stable fixed-point. *Neural Computation*, *16*(5), 885–940.
- Chechik, G. (2003). Spike-timing-dependent plasticity and relevant mutual information maximization. *Neural Computation*, *15*, 1481–1510.
- Dan, Y., & Poo, M.-m. (2004, September). Spike timing-dependent plasticity of neural circuits. *Neuron*, *44*, 23–30.
- Dayan, P. (2002, March). Matters temporal. *TRENDS in Cognitive Sciences*, *6*(3), 105–106.
- Dayan, P., & Häusser, M. (2004). Plasticity kernels and temporal statistics. In S. Thrun, L. Saul, & B. Schölkopf (Eds.), *Advances in neural information processing systems 16*. Cambridge, MA: MIT Press.
- Debanne, D., Gähwiler, B., & Thompson, S. (1998). Long-term synaptic plasticity between pairs of individual ca3 pyramidal cells in rat hippocampal slice cultures. *J. Physiol.*, *507*, 237–247.
- Feldman, D. (2000, July). Timing-based ltp and ltd at vertical inputs to layer ii/iii pyramidal cells in rat barrel cortex. *Neuron*, *27*, 45–56.
- Froemke, R., & Dan, Y. (2002). Spike-timing-dependent synaptic modification induced by natural spike trains. *Nature*, *416*, 433–438.
- Gerstner, W. (2001). A framework for spiking neuron models: The spike response model. In F. Moss

- & S. Gielen (Eds.), *The handbook of biological physics* (Vol. 4, p. 469-516).
- Gerstner, W., Kempter, R., van Hemmen, J. L., & Wagner, H. (1996). A neural learning rule for sub-millisecond temporal coding. *Nature*, 383, 76–78.
- Gerstner, W., & Kistler, W. (2002). *Spiking neuron models*. Cambridge, UK: Cambridge University Press.
- Hennion, P. E. (1962, April). Algorithm 84: Simpson's integration. *Communications of the ACM*, 5(4), 208.
- Herrmann, A., & Gerstner, W. (2001). Noise and the PSTH response to current transients: I. General theory and application to the integrate-and-fire neuron. *J. Comp. Neurosci.*, 11, 135–151.
- Hopfield, J., & Brody, C. (2004). Learning rules and network repair in spike-timing-based computation. *PNAS*, 101(1), 337–342.
- Izhikevich, E., & Desai, N. (2003). Relating stdp to bcm. *Neural Computation*, 15, 1511–1523.
- Jolivet, R., Lewis, T., & Gerstner, W. (2003). The spike response model: a framework to predict neuronal spike trains. In K. et al. (Ed.), *Proc. joint international conference icann/iconip 2003* (pp. 846–853). Springer, LNCS 2714.
- Kandel, E. R., Schwartz, J., & Jessell, T. M. (2000). *Principles of neural science*. Mc Graw Hill.
- Karmarkar, U., Najarian, M., & Buonomano, D. (2002). Mechanisms and significance of spike-timing dependent plasticity. *Biol. Cybern.*, 87, 373–382.
- Kempter, R., Gerstner, W., & van Hemmen, J. (1999). Hebbian learning and spiking neurons. *Phys. Rev. E*, 59(4), 4498–4514.
- Kempter, R., Gerstner, W., & van Hemmen, J. (2001). Intrinsic stabilization of output rates by spike-based hebbian learning. *Neural Computation*, 13, 2709–2742.
- Kepecs, A., van Rossum, M., Song, S., & Tegner, J. (2002). Spike-timing-dependent plasticity: common themes and divergent vistas. *Biol. Cybern.*, 87, 446–458.
- Legenstein, R., Naeger, C., & Maass, W. (n.d.). *What can a neuron learn with spike-timing-dependent plasticity?* (submitted)
- Markram, H., Lübke, J., Frotscher, M., & Sakmann, B. (1997). Regulation of synaptic efficacy by coincidence of postsynaptic apss and epsps. *Science*, 275, 213–215.
- Nishiyama, M., Hong, K., Mikoshiba, K., Poo, M.-m., & Kato, K. (2000, Nov). Calcium stores regulate the polarity and input specificity of synaptic modification. *Nature*, 408, 584–588.
- Paninski, L., Pillow, J., & Simoncelli, E. (2005). Comparing integrate-and-fire models estimated using intracellular and extracellular data. *Neurocomputing*. (to appear)
- Porr, B., & Wörgötter, F. (2003). Isotropic sequence order learning. *Neural Computation*, 15(4), 831–864.
- Rao, R., & Sejnowski, T. (1999). Predictive sequence learning in recurrent neocortical circuits. In T. L. S. Solla & K. Muller (Eds.), *Advances in neural information processing systems 12* (pp. 164–170). Cambridge, MA: MIT Press.
- Rao, R., & Sejnowski, T. (2001). Spike-timing-dependent plasticity as temporal difference learning. *Neural Computation*, 13, 2221–2237.
- Roberts, P., & Bell, C. (2002, Dec). Spike timing dependent synaptic plasticity in biological systems. *Biol. Cybern.*, 87, 392–403.
- Saudargiene, A., Porr, B., & Wörgötter, F. (2004). How the shape of pre- and postsynaptic signals can influence stdp: A biophysical model. *Neural Computation*, 16, 595–625.
- Senn, W., Markram, H., & Tsodyks, M. (2000). An algorithm for modifying neurotransmitter release probability based on pre- and postsynaptic spike timing. *Neural Computation*, 13, 35–67.
- Shon, A., Rao, R., & Sejnowski, T. (2004). Motion detection and prediction through spike-timing dependent plasticity. *Network: Comput. Neural Syst.*, 15, 179–198.
- Sjöström, P., Turrigiano, G., & Nelson, S. (2001, December). Rate, timing, and cooperativity jointly determine cortical synaptic plasticity. *Neuron*, 32, 1149–1164.
- Song, S., Miller, K., & Abbott, L. (2000). Competitive hebbian learning through spike-time-dependent synaptic plasticity. *Nature Neuroscience*, 3, 919–926.

- Toyoizumi, T., Pfister, J.-P., Aihara, K., & Gerstner, W. (2005). Spike-timing dependent plasticity and mutual information maximization for a spiking neuron model. In *Advances in neural information processing systems 17*. MIT Press.
- van Rossum, R., Bi, G.-q., & Turrigiano, G. (2000). Stable hebbian learning from spike time dependent plasticity. *J. Neurosci.*, *20*, 8812–8821.
- Xie, X., & Seung, H. (2004). Learning in neural networks by reinforcement of irregular spiking. *Physical Review E*, *69*(041909).
- Zhang, L., Tao, H., Holt, C., Harris, W., & Poo, M.-m. (1998). A critical window for cooperation and competition among developing retinotectal synapses. *Nature*, *395*, 37–44.